Heat and Moisture Budgets during the Period of HUBEX/GAME in the Summer of 1998

PENG Jingbei (彭京备) and SONG Zhengshan (宋正山)

Institute of Atmospheric Physics, Chinese Academy of Sciences, Beijing, 100029

(Received January 18, 2002; revised November 22, 2002)

ABSTRACT

By using the high-resolution GAME reanalysis data, the heat and moisture budgets during the period of HUBEX/GAME in the summer of 1998 are calculated for exploring the thermodynamic features of Meiyu over the Changjiang-Huaihe (CH) valley. During the CH Meiyu period, an intensive vertically-integrated heat source and moisture sink are predominant over the heavy rainfall area of the CH valley, accompanied by strong upward motion at 500 hPa. The heat and moisture budgets show that the main diabatic heating component is condensation latent heat released by rainfall. As residual terms, the evaporation and sensible heating are relatively small. Based on the vertical distribution of the heat source and moisture sink, the nature of the rainfall is mixed, in which the convective rainfall is dominant with a considerable percentage of continuous stratiform rainfall. There are similar time evolutions of the main physical parameters ($\langle Q_1 \rangle$, $\langle Q_2 \rangle$, and vertical motion ω at 500 hPa). The time variations of $\langle Q_1 \rangle$ and $\langle Q_2 \rangle$ are in phase with those of $-\omega_{500}$, and have their main peaks within the CH Meiyu period. This shows the influence of the heat source on the dynamic structure of the atmosphere. The wavelet analyses of those time series display similar multiple timescale characteristics. During the CH Meiyu period, both the synoptic scale(~6 days) and mesoscale (~2 days and ~12 hours) increase obviously and cause heavy rainfall as well as the appearances of the maxima of the main physical parameters. Among them, the mesoscale systems are the main factors.

Key words: heat and moisture budgets, Meiyu, the Changjiang-Huaihe valley, HUBEX, multiple timescale

1. Introduction

A series of studies have been performed concerning the heat and moisture budgets over East China and surrounding regions in summer, including large-scale characteristics of spatial and temporal distribution of heat sources and moisture sinks in different years (Johnson et al., 1993; Yanai et al., 1992; Luo and Yanai, 1984; Ding and Wang, 1988; Ding and Hu, 1988). Recently, some characteristics of heat and moisture budgets over the area of Changjiang (CJ) and the Huaihe Valley in the summers of 1998 and 1999 have been explored further by utilizing the lower-resolution NCEP/NCAR dataset (Song et al., 2001; Peng and Song, 2001; Ding et al., 2001). Because 1998 and 1999 are two flood years over CJ and the Huaihe Valley, all the studies are valuable for understanding the formation and maintenance mechanism of anomalous climate.

The years 1998 and 1999 are HUBEX/GAME years too, in which intensive field observations over East China were conducted (Zhao and Ding, 1999). In particular, other than HUBEX/GAME, intensive field observations were carried out in other GAME regions from April to September 1998. Based on these observations, a high-resolution gridded dataset of meteorological elements has been constructed. It is worthwhile to recalculate the heat and moisture budgets associated with Meiyu over the Changjiang-Huaihe (CH) valley in order to obtain more accurate and reasonable results by using the high-resolution GAME dataset. In this paper, we give some new results concerning the temporal and spatial characteristics of the heat and moisture budgets in the summer of 1998.

The dataset and method of analysis are presented in section 2. Section 3 describes the rainfall and large-scale circulation of the CH Meiyu. Section 4 discusses the heat source and moisture sink budgets during the CH Meiyu period. Section 5 illustrates the multiple timescale characteristics of the main physical parameters. The main conclusions are summarized in section 6.

*E-mail: jingbeipeng@hotmail.com

2. Data and method of analysis

The dataset used in this study is the high-resolution GAME reanalysis dataset, version 1.1 from 15 June to 15 July 1998 in the domain 30°–180°E, 30°–80°N, provided by the Meteorological Research Institute of Japan. It includes:

1) The 6-hourly upper air reanalysis data at 17 levels (1000, 925, 850, 700, 600, 500, 400, 300, 250, 200, 150, 100, 70, 50, 30, 20, 10 hPa), with 0.5°×0.5° horizontal resolution.

2) Latent and sensible heat flux by 2-dimensonal forecast fields with 1.25°×1.25° horizontal resolution.

In addition, the 6-hourly rainfall records of 35 stations over the CH valley for the same period, provided by the National Climate Center of China, are also used.

The apparent heat source Q_1 and the apparent moisture sink Q_2 are computed by the following equations (Yanai et al., 1992):

$$Q_1 = c_p \left(\frac{p}{p_0}\right)^{\kappa} \left(\frac{\partial \theta}{\partial t} + \boldsymbol{V} \cdot \nabla \theta + \omega \frac{\partial \theta}{\partial p}\right), \quad (1)$$

$$Q_2 = -L \left(\frac{\partial q}{\partial t} + \boldsymbol{V} \cdot \nabla q + \omega \frac{\partial q}{\partial p}\right), \quad (2)$$

where the symbols are as normally used. Vertical p-velocity ω is obtained from the horizontal divergence by vertically integrating the continuity equation. The upper and lower boundary conditions are determined by Equation (1) and the forcing effects of topography respectively.

By integrating (1) and (2) from the tropopause pressure p_T to the surface pressure p_s, we obtain

$$\langle Q_1 \rangle = \frac{1}{g} \int_{p_T}^{p_s} Q_1 dp = \langle Q_R \rangle + LP + S, \quad (3)$$

$$\langle Q_2 \rangle = \frac{1}{g} \int_{p_T}^{p_s} Q_2 dp = L(P - E), \quad (4)$$

where $\langle Q_R \rangle$ is the radiative heating rate and P, S, and E are the precipitation rate, the sensible heat flux, and the evaporation rate per unit area at the surface, respectively.

During the period of Meiyu in 1998, various scales of precipitating systems form and develop. The Morlet wavelet is adapted to the time series of the main physical parameters to reveal their multiple timescale characteristics. The expressions of the Morlet wavelet are as follows:

$$g(t) = e^{ict} e^{-t^2/2}, \quad (5)$$

$$g_{ab}(t) = \frac{1}{\sqrt{a}} g\left(\frac{t-b}{a}\right), \quad (6)$$

where a, b are real and $a0$. The wavelet transform (WT) of the time series $f(t)$ is the inner product of $f(t)$ and $g_{ab}(t)$:

$$T_g(a,b) = \frac{1}{\sqrt{a}} \int g\left(\frac{t-b}{a}\right) f(t)\, dt. \quad (7)$$

Taking c=6.2306, the dilation parameter a corresponds to the period in the Fourier transform (Meyer et al., 1993).

According to the distribution of the main rainfall center, a special region A (111°–119°E, 30°–34°N) of the CH valley (Fig. 1) has been selected for obtaining area-averaged values of the main physical parameters concerned. The domain of area A corresponds to the β-scale observational sub-region settled by HUBEX.

3. Rainfall and large scale circulation of CH Meiyu

Ding et al. (2001) described the evolution of large-scale circulation and the rainfall processes associated with the Meiyu in 1998. The rainfall in the summer of 1998 is special and can be divided into three sub-periods:

Period I (1st CJ Meiyu): Heavy rainfall appears in southern area of the CJ River from 11 June to 27 June.

Period II (CH Meiyu): Heavy rainfall is over the CH valley from 28 June to 3 July.

Period III (2nd CJ Meiyu): Heavy rainfall occurs again over the CJ valley from 16 July to the beginning of the next month.

The distribution of the total rainfall amount of the CH Meiyu (Fig. 1) shows that the center of the rainfall (> 800 mm) is just located over the CH valley with a much larger rainfall rate than before or after the CH Meiyu period (Fig. 2).

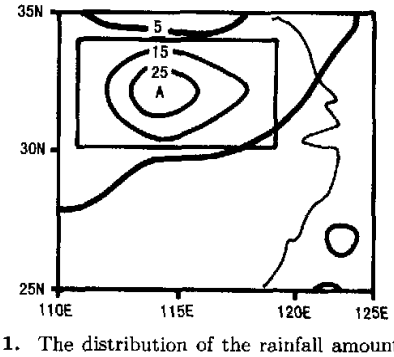

Fig. 1. The distribution of the rainfall amount of the CH Meiyu in 1998. The area A (111°–119°E, 30°–34°N) in the CH valley is for obtaining the area-averaged values of the physical parameters. Unit: mm d^{-1}.

The HUBEX/GAME experiment with intensive particular observations focuses on the CH valley Meiyu (Period II), during which the circulation situation at 500 hPa displays a kind of typical Meiyu pattern "two troughs and one ridge" (Fig. 3). A high ridge stays over the Lake Baikal with a trough on each side. The ridge of the subtropical high over the Western Pacific Ocean is along 27°N. The northwest flow (cold and dry) between the Lake Baikal ridge and the downstream cold trough merges with the southwest flow (warm and wet) in the western periphery of the subtropical high to form the strong westerly belt extending from eastern China to Japan. Several vortex systems in the lower levels propagate eastward just along the south side of the westerly belt and bring the heavy rainfall of Meiyu over the CH valley (Fig. 3).

Such a circulation situation is destroyed after the Lake Baikal ridge is replaced by a trough, and the subtropical high migrates northward with its axis along 30°N after 4 July resulting in the end of the CH Meiyu.

4. The heat and moisture budgets

a) The horizontal distribution of $\langle Q_1 \rangle$, $\langle Q_2 \rangle$ and ω at 500 hPa

The mean horizontal distributions of $\langle Q_1 \rangle$, $\langle Q_2 \rangle$, and ω at 500 hPa (ω_{500}) for the CH Meiyu period are shown in Fig. 4. The whole of eastern China is a heat source with the center (~800 W m^2) just over the heavy rainfall area of the CH basin. The distribution of $\langle Q_2 \rangle$ is quite similar to that of $\langle Q_1 \rangle$ in pattern and intensity of the center, indicating the dominant role of condensation heating caused by Meiyu rainfall.

The positive regions of $\langle Q_1 \rangle$, $\langle Q_2 \rangle$ are accompanied by an area of strong upward motion, showing the influence of the heat source on the dynamic structure of the atmosphere. These features are consistent with the results obtained by other studies for several flood years in the CH Valley (Johnson et al., 1993; Yanai et al., 1992; Ding and Wang, 1988; Ding and Hu, 1988; Ding et al., 2001; Song and Peng, 2001; Peng and Song, 2001).

b) Mean vertical profiles of Q_1, Q_2, and ω

Careful study of the vertical distributions of Q_1 and Q_2 yields valuable information on the nature of the heating processes. Figure 5 shows the vertical profiles of the area-averaged heating-rate Q_1/c_p, drying rate Q_2/c_p, and ω for the CH Meiyu period. The vertical motions are upward with a peak value (~−7 hPa h^{-1}) between 400–500 hPa.

The heating rate Q_1/c_p has its maximum (~11K d^{-1}) at 500 hPa, but the maximum of Q_2/c_p (~10 K d^{-1}) appears at a slightly lower level (~600 hPa).

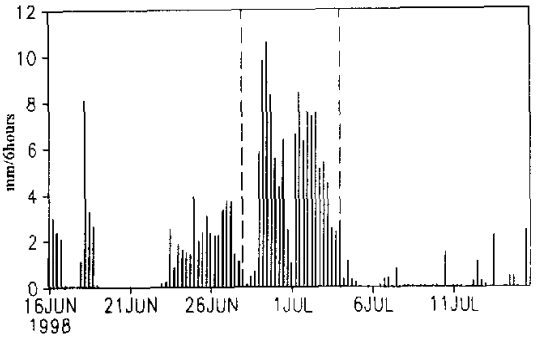

Fig. 2. The time variation of area-averaged rainfall amount from 15 June to 15 July 1998. Dashed line denotes the period of the CH Meiyu in 1998. Units: mm 6 h^{-1}.

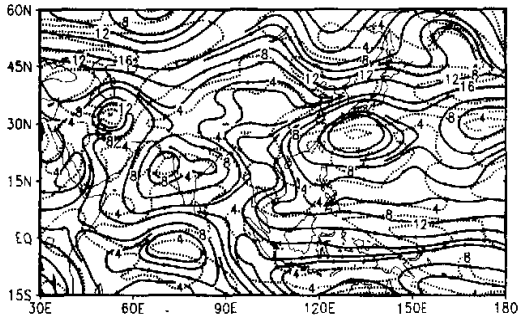

Fig. 3. Mean winds at 500 hPa for the CH Meiyu period in 1998. Isotachs are drawn at 4 m s^{-1}. The ground surfaces above 3000 m are shaded.

The rate Q_1/c_p is smaller than the rate Q_2/c_p in the lower troposphere, while the reverse is true in the upper troposphere, reflecting the effects of deep cumulus convection as pointed out by Luo and Yanai (1984).

It should be noted that the profiles of Q_1/c_p and Q_2/c_p are close to each other with small separation of peak heights, suggesting the coexistence of convective precipitation and considerable stratiform cloud. Therefore, the nature of rainfall of the CH Meiyu was the combination of convective and continuous precipitation.

c) The total heat and moisture balances

Based on Equations (3) and (4), the total heat and moisture balances averaged over area A for the CH Meiyu period are calculated (Table 1). The LP is obtained by using routine observation of precipitation. The value of $\langle Q_R \rangle$ is taken as the climatic mean (−95

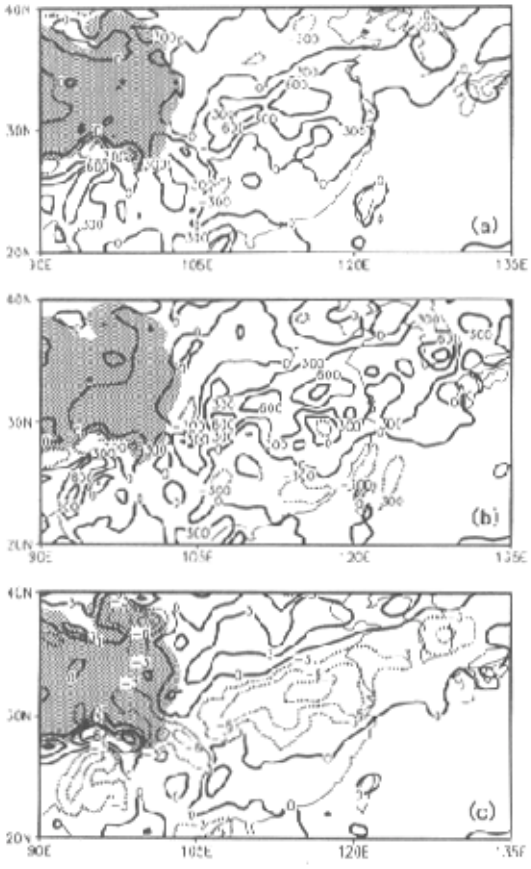

Fig. 4. Mean horizontal distribution of (a) $\langle Q_1 \rangle$, (b) $\langle Q_2 \rangle$ and (c) ω_{500} for the CH Meiyu period in 1998. Units: $\langle Q_1 \rangle$, $\langle Q_2 \rangle$, W m^{-2}; ω_{500}: hPa h^{-1}.

W m^{-2}) used by Nitta (1983). Quantities S and LE are estimated as residuals of Equations (3) and (4).

Due to the heavy rainfall in the CH Meiyu, the condensation term LP is very large and reaches 555 W m^{-2}. The values of $\langle Q_1 \rangle$ and $\langle Q_2 \rangle$ calculated by means of vertically integrating Equations (1) and (2) are 487 and 505 W m^{-2} respectively. These values are close to that of LP, indicating again the importance of the release of condensation latent heat for heat and moisture budgets. As the residuals of Equations (3) and (4), S and LE are much smaller with values of only 27 W m^{-2} and 50 W m^{-2} respectively. This can be attributed to the high air humidity and the lack of sunshine in the period of the CH Meiyu.

The above-estimated S and LE are compared with those by the GAME 2-dimensional forecast fields in which the S and LE are given as 16 W m^{-2} and 64 W m^{-2} respectively. The sets of values are comparable to each other and illustrates the reasonability of the estimated S and LE. But the estimated LE is much smaller than that by Bowen Ratio-Energy Balance and Eddy Correlation methods however. By these methods, the LE is about 300 W m^{-2} for June-July 1998 at Shouxian County of Anhui Province, based on the boundary layer observation data of HUBEX (Zhu et al., 1999). Due to the importance of the parameter LE for heat and moisture budgets, further study is necessary for obtaining a more reasonable estimation.

Table 1. Total heat and moisture balances for the CH Meiyu period in 1998(W m^{-2})

Heat balance				Moisture balance		
$\langle Q_1 \rangle$	$\langle Q_R \rangle$	LP	S	$\langle Q_2 \rangle$	LP	LE
487	−95	555	27	505	555	50

5. The time variations and multi-scale characteristics of $\langle Q_1 \rangle$, $\langle Q_2 \rangle$, and ω_{500}

Figure 6 shows time variations of $\langle Q_1 \rangle$, $\langle Q_2 \rangle$, and ω_{500} averaged over area A of the CH valley. Since the onset of the CH Meiyu (28 June), $\langle Q_1 \rangle$ increases obviously from a relatively small value and reaches its peak on 29 June. After weakening for a short period around 30 June, it grows again and remains until the end of the CH Meiyu. After 3 July, $\langle Q_1 \rangle$ decreases quickly.

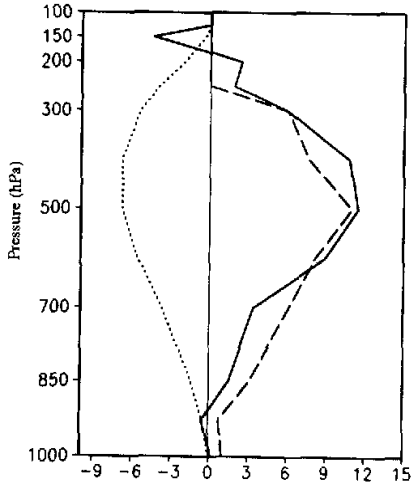

Fig. 5. Vertical profiles of area-averaged Q_1/c_p (solid), Q_2/c_p (dashed), and ω (point) for the CH Meiyu period in 1998. Units: Q_1, Q_2: K d^{-1}; ω: hPa h^{-1}.

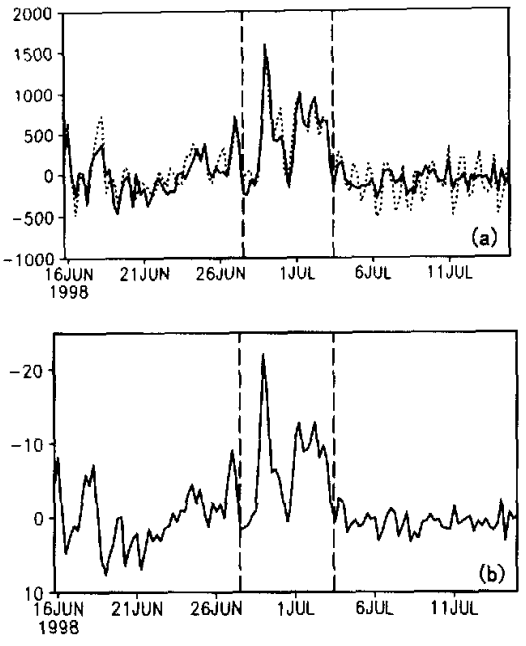

Fig. 6. Time series of area-averaged (a) $\langle Q_1 \rangle$ (solid) and $\langle Q_2 \rangle$ (dashed) and (b) ω_{500}. Units: $\langle Q_1 \rangle$, $\langle Q_2 \rangle$: W m^{-2}; ω: hPa h^{-1}.

Compared with the evolution of rainfall (Fig. 2), the main peaks of $\langle Q_1 \rangle$ correspond to those of the rainfall. The temporal variations of $\langle Q_2 \rangle$ are similar to those of $\langle Q_1 \rangle$ not only in variation tendency but also in intensity, indicating that the variation of the heating is mainly due to the latent heat release.

The fluctuation of $-\omega_{500}$ is in phase with those of $\langle Q_1 \rangle$ and $\langle Q_2 \rangle$. Before and after the Meiyu period, the vertical motion is relatively weak and downward motion is observed often. But strong upward motion appears from 28 June and reaches its maximum on 29 June. Then, it intensifies to a secondary maximum on June 30. The peaks of $\langle Q_1 \rangle$ and $\langle Q_2 \rangle$ coincide with those of $-\omega_{500}$, indicating the influence of the heat source on the dynamic structure of atmosphere.

The multiple timescale characteristics of the time series of these physical parameters are displayed in Fig. 7. There are two kinds of dominant timescale fluctuations pronounced in different periods:

(i) Synoptic scale (~6 days)

The ~6-day synoptic scale fluctuations are dominant throughout the whole analysis period, but the activity reaches its maximum just within the CH Meiyu period . The active scales increase toward longer periods from 5 days to 7 days before the end of the CH Meiyu, then maintain a period of ~6 days and the activity weakens gradually.

The ~6-days synoptic scale fluctuations in the CH Meiyu period are connected closely with the evolution of the large scale circulation, as described in section 3.

(ii) Mesoscale (less than ~3 days)

The ~2-day mesoscale fluctuations are active on 16–18 June within the Period I (1st CJ Meiyu) in 1998. Another active period is from 24 June to 6 July. The activity grows obviously throughout whole CH Meiyu period and reaches a maximaum on 28–29 June with an increasing time-scale trend thereafter. A notable phenomenon is that the shorter fluctuations, whose period is about 12 hours (semidiurnal), are pronounced only within the period of the CH Meiyu. They are stronger on 28–29 June, but very weak, except the CH Meiyu period.

Therefore, several systems with different timescales coexist within the CH Meiyu period and interact in a complex manner. The mesoscale systems intensify along with the development of the synoptic scale systems, which causes heavy rainfall (convective and continuous) and the appearance of the maxima of the main physical parameters. The synoptic scale systems constitute the environmental background condition favorable to the development of mesoscale systems and are responsible for the stratiform rainfall. But the mesoscale systems are the main factor in the heavy rainfall of the CH Meiyu.

The activities of mesoscale systems in the period of the CH Meiyu are detected by the Doppler radar observations of HUBEX. Several mesoscale convective systems have formed and developed within the stratiform cloud rainfall system in the Huaihe River Basin on 29 June 1998 (Geng et al., 2000).

6. Summary

The major findings on the CH Meiyu of 1998 in this study can be summarized as followings.

1) The horizontal distributions of $\langle Q_1 \rangle$ and $\langle Q_2 \rangle$ show that the centers of heat sources and moisture sinks, all about 800 W m^{-2}, appear over the area of the CH valley and coincide with those of the heavy rainfall and upward motion centers.

2) Area-averaged $\langle Q_1 \rangle$, $\langle Q_2 \rangle$, and LP reached 487, 505, and 555 W m^{-2}, respectively, showing that the main heating factor is the release of condensation latent heat associated with heavy rainfall.

3) As the residual terms in the budget equations, the estimated evaporation and sensible flux from the surface are smaller and consistent with those given by the GAME dataset.

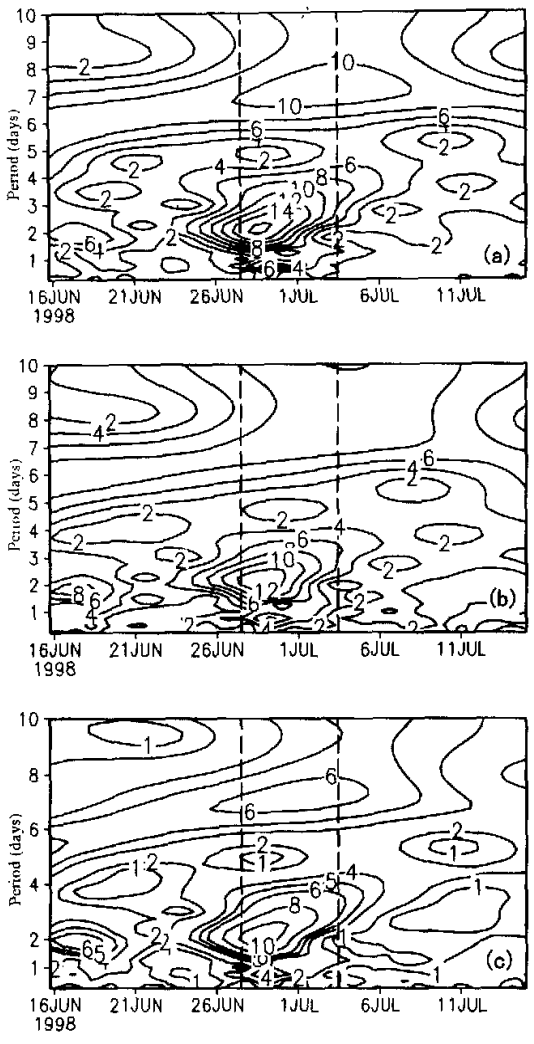

Fig. 7. The mode of the wavelet transform for area-averaged (a) $\langle Q_1 \rangle$, (b) $\langle Q_2 \rangle$ and (c) ω_{500}. Units: $\langle Q_1 \rangle$, $\langle Q_2 \rangle$: W m^{-2}; ω_{500}: hPa h^{-1}.

4) The vertical profiles of area-averaged $\langle Q_1 \rangle$ and $\langle Q_2 \rangle$ show that both convective and stratiform precipitations are in the CH Meiyu.

5) The time variations of $\langle Q_1 \rangle$, and $\langle Q_2 \rangle$ are in phase with those of $-\omega_{500}$. After the beginning of the Meiyu, they increase and reach their peaks at 29 June. But other than in the Meiyu period, $\langle Q_1 \rangle$, $\langle Q_2 \rangle$, and ω_{500} are small.

6) The wavelet transform is applied to the time series of $\langle Q_1 \rangle$, $\langle Q_2 \rangle$, and ω_{500} for examining the characteristics of multiple timescales. During the Meiyu period, the activity of the synoptic scale (~6days) reaches a maximum, and the mesoscale fluctuations (periods of ~2 days and ~12 hours) are pronounced. The mesoscale disturbances are the main factors in causing the heavy rainfall as well as the appearances of the maxima of the main physical parameters.

The results obtained in this study are preliminary. The advantage in using the high-resolution GAME reanalysis data is evident. The calculated heat source, moisture sink, and vertical motion display rather larger values compared to using the NCEP/NCAR reanalysis data with lower resolution, but the values seem to be more reasonable in estimating the heat and moisture balances (Song and Peng, 2001; Ding et al., 2001). In particular, more details of the activities of mesoscale disturbances can be explored by using high-resolution data. Due to the limitation of time resolution, it is impossible to find disturbances with the time scale of ~12 hours by using low-resolution data. Because of the complexity of the CH Meiyu processes, more extensive research is necessary in the future.

Acknowledgments. This work was supported by the National Natural Science Foundation of China under Grant No. 497914030.

REFERENCES

Ding Y. H., and Hu J., 1988: The variation of the heat sources in East China in the early summer of 1984 and their effects on the large-scale circulation in East Asia. *Advances in Atmospheric Sciences.* **5**, 171–180.

Ding Y. H., and Wang X. F., 1988: An analysis of the distribution of apparent heat sources and sinks over the middle reaches of Yangtze River during the Meiyu season in 1983. *Tropical Meteorology*, 4, 134-145. (in Chinese)

Ding, Y.-H., Zhang Y., Ma Q., and Hu G. Q., 2001: Analysis of the large-scale circulation features and synoptic systems in East Asia during the intensive observation period of HUBEX/GAME. *J. Meteor. Soc. Japan*, **79**, 277–300.

Geng, B., K. Tsuboki, T. Takeda, Y. Fujiyoshi, and H. Uyeda, 2000: Relationship between middle-level inflow and organization of mesoscale convective system. International GAME/HUBEX Workshop, Sapporo, 65–68.

Johnson, R. H., Z. Wang, and J. F. Bresch, 1993: Heat and moisture budgets over China during the early summer monsoon. *J. Meteor. Soc. Japan*, **71**, 137–151.

Luo, H. -B., and M. Yanai, 1984: The large-scale circulation and heat sources over the Tibetan Plateau and surrounding areas during the early summer of 1979. Part II: Heat and moisture budgets. *Mon. Wea. Rev.*, **112**, 966–989.

Meyers, S. D., B. G. Kelly, and J. J. O'Brien, 1993: An introduction to wavelet analysis in oceanography and meteorology: With application to the dispersion of Yanai waves. *Mon. Wea. Rev.*, **121**, 2858–2866.

Nitta, T., 1983: Observational study of heat source over the eastern Tibetan Plateau during the summer monsoon. *J. Meteor. Soc. Japan*, **61**, 590–605.

Peng J. B., and Song Z. S., 2001: The characteristics of temporal and spatial variations of heat sources, moisture sinks over the Changjiang-Huaihe valley in summer 1999. *Climatic and Environmental Research*, **6**, 153–160. (in Chinese)

Song Z. S., and Peng J. B., 2001: The heat, moisture budgets and their multiple timescale features over Jiang-Huai Valley during Meiyu period of 1998. *Polar Invasion and Typhoon and Damage*, Qiu Y. Y., Eds., China Meteorological Press, 576–588. (in Chinese)

Yanai, M., C. F. Li, and Z. S. Song, 1992: Seasonal heating of the Tibetan Plateau and its effects on the evolution of the Asian summer monsoon. *J. Meteor. Soc.* Japan, **70**, 319–350.

Zhao B. L., and Ding Y. H. (Eds.), 1999: *Study of Energy and Water Cycle over Huaihe River Basin (I)*. China Meteorological Press, 273 pp. (in Chinese)

Zhu Z. L., Sun X. M., and Zhang R. H., 1999: Experimental study on the estimate of energy balance in Huaihe River Basin using micrometeorological methods. *Study of Energy and Water Cycle over Huaihe River Basin (I)*, Zhao Bolin and Ding Yihui, Eds., China Meteorological Press, 144–152. (in Chinese)

1998年夏季HUBEX/GAME期间热量和水汽收支

彭京备　宋正山

摘　要

使用1998年夏季高分辨率的GAME再分析资料，通过计算热量和水汽收支，分析了江淮梅雨的热力和动力特征。梅雨期间，江淮整个地区为强热源及水汽汇控制，並伴有强上升运动。热量和水汽收支计算表明，非绝热加热主要是降水产生的凝结潜热释放，地面感热和蒸发耗热均较小。江淮梅雨降水是对流云和层状云共同产生的混合性降水。子波分析显示，热源、水汽汇和垂直运动有相似的时间变化和多尺度特征。江淮梅雨期间，周期约为6天的天气尺度扰动以及周期约为2天和12小时的中尺度扰动同时发展，使江淮地区产生暴雨，並引起了热源、水汽汇和上升运动的最大值，对此中尺度扰动起了主要作用。

关键词: 热量和水汽收支，梅雨，江淮流域，HUBEX，多时间尺度